The Astrophysical Journal, 591:784–790, 2003 July 10
© 2003. The American Astronomical Society. All rights reserved. Printed in U.S.A.

DARK AND LUMINOUS MATTER CONNECTIONS FROM SMOOTHED PARTICLE HYDRODYNAMIC SIMULATIONS OF ISOLATED TRIAXIAL COLLAPSING SYSTEMS

P. Mazzei
Instituto Nazionale di Astrofisica, Astronomy Observatory, Padova, Vicolo dell' Osservatorio 5, 35122 Padua, Italy; mazzei@pd.astro.it

and

A. Curir
Instituto Nazionale di Astrofisica, Astronomy Observatory, Pino Torinese, Strada Osservatorio 20, 10025 Turin, Italy
Received 2002 November 27; accepted 2003 March 20

ABSTRACT

We performed smoothed particle hydrodynamic simulations of isolated collapsing triaxial systems initially composed of dark matter and gas with cooling, shocks, star formation, and feedback, in particular, self-consistently accounted for. We aim to shed light on the dependence of system evolution on some parameters so far unexplored, such as total mass, initial geometry, and dynamical state. Moreover, the effects of different values of the baryonic–to–total mass ratio have been investigated. We find intriguing connections between dark and luminous matter. The initial properties of the halo drive galaxy formation and evolution. We point out important issues concerning galaxy morphological types. In our framework, spiral galaxies arise only in systems with both a total mass lower than $10^{12}\ M_{\odot}$ and a critical value of the baryonic–to–total mass ratio around 0.1. For the same value of such a ratio, the more massive systems host massive elliptical galaxies as a consequence of the stronger bursts of star formation arising into their halos. Higher values of such a ratio provide baryons with lower rotational support so that no constraints on the total mass of the system hosting an elliptical galaxy have been derived.

Subject headings: galaxies: evolution — galaxies: formation — galaxies: fundamental parameters — galaxies: halos — methods: numerical

On-line material: color figures

1. INTRODUCTION

The past two decades have witnessed the emergence of a successful class of theoretical models that explain the formation of the structures in the universe. Hierarchical clustering is currently the most successful paradigm of structures formation. Numerical simulations have become an important tool for exploring the detailed predictions of these models. However, extending these studies to understand the formation of luminous components of galaxies is difficult since our knowledge of the star formation (SF) process and its interaction (feedback) with the surrounding interstellar medium is still rather limited. Moreover, computational resources strongly constrain their baryonic resolution; thus, most of the simulations that focus on the formation of individual galaxies are not performed in a cosmological scenario (Katz, Hernquist, & Weinberg 1992; Katz, Weinberg, & Hernquist 1996; Barnes & Hernquist 1991; Springel 2000). In this context, we (Curir & Mazzei 1999, hereafter Paper I) were the first to present results from smoothed particle hydrodynamic (SPH) simulations of isolated collapsing triaxial systems, initially composed of dark matter (DM) and gas and with the SF switched on, implemented with chemophotometric evolutionary population synthesis (EPS) models providing the spectral energy distribution from UV up to the near-infrared K band. We have focused on the final properties of these systems, i.e., after 15 Gyr in the rest frame, for different values of the stellar initial mass function (IMF) parameters [i.e., $\phi(M) \propto M^{-\alpha}$, where α is slope and $M_{\rm low}$ is lower mass limit] and feedback strengths are self-consistently accounted for (see § 2.1). Colors and metallicities of our simulated galaxies are fully consistent with those of local ones (see Paper I, Fig. 11). We point out important evolutionary trends of these kind of models to shed light into several problems completely unexplored until now. To do so, we performed a large set of new simulations (§ 2.2). Here we present the time behavior of both the star formation rate (SFR) and the rotational support (the ratio between rotational to kinetic energy) of the baryons (gas+stars) provided by these simulations to derive some issue concerning galaxy morphological types and their dependence on the properties of the whole system, particularly of their DM halos. We find that the total mass of the system, the DM halo initial geometry given by different values of initial triaxiality ratio (see § 2.2) and its dynamical state, strongly reflect on galaxy formation and evolution. Moreover, we outline the effect of different values of the baryonic–to–total mass ratio ($M_{\rm bar}/M_{\rm tot}$; see § 3), showing that its cosmological value, around 0.1, coupled with the less massive halos ($M \leq 10^{12}\ M_{\odot}$), strongly favors the formation of a disk galaxy as obtained in a fully consistent cosmological scenario (Steinmetz & Navarro 2002). Our findings represent a deepening of galaxy formation problems that have begun to be investigated very recently (Abadi et al. 2002; Governato et al. 2002). We believe that our work will be improved by the next generation of fully consistent cosmological simulations of galaxy formation. In § 2, we present our recipes to include SF and feedback and summarize the initial configuration of the system widely discussed in Paper I. In § 3, we present and discuss the results, and in § 4, we present our conclusions.

2. RECIPES

Following the pioneering work of White & Rees (1978), one of the critical processes during galaxy formation is

radiative cooling. Cosmological hydrodynamical simulations show that all the gas in virialized systems cools at the center in a runaway process (overcooling), which can be halted if (1) a large fraction is transformed into stars, (2) most of the gas settles in a rotationally supported disk, or (3) some energy input reheats the gas (Navarro & White 1994). Therefore, since our understanding of the SF process and its interaction with the surrounding interstellar medium is still rather limited, simulations including such a process are made on the basis of a phenomenological approach that translates into a power-law dependence of the SFR on the local gas density. In all cases, the basic procedure is the same: at the end of each time step, a subset of gas particles is being identified as eligible to form stars. A fraction of the particles are then converted into stars, which are subsequently subject only to gravitational interactions. In a recent study, Kay et al. (2002) analyze the effect of different SF recipes in N-body/SPH cosmological simulations of galaxy formation. The reader is referred to the exhaustive discussion on this topic presented in that paper for more details. The star-forming criterion adopted here is developed on the basis of the following conditions (Navarro & White 1993): (1) The local gas density must be larger than a threshold value, 7×10^{-26} g cm^{-3}, which corresponds to the Jeans instability criterion and to a cooling time shorter than dynamical time in the region. (2) The gas particle must be in a convergent flux, i.e., $\Delta v < 0$, so pressure forces are unable to stop the collapse. A gas particle satisfying these conditions loses a fraction ϵ of its mass, which becomes a star particle. Kay et al. (2002) conclude that results do not depend strongly on different SFR prescriptions when feedback is neglected: the ratio of cold gas to stars in the final galaxy is primarily controlled by the range of gas density where the SF is allowed to proceed efficiently. However, even with SF inclusion, the fraction of gas that cools is much too high to account for the K-band luminosity function, so feedback must be accounted for. Therefore, once stars are present, they are expected to return to the interstellar medium (ISM) part of their mass and energy via supernovae (SNe) explosions, stellar winds, and UV flux. These latter contributions are relevant only for massive stars. All this is known as stellar energy feedback. There are two ways of including phenomenological feedback models in cosmological simulations: thermal (Katz 1992) and kinetic. In the former case, all the energy (from SNe, stellar winds, and UV flux) supplies the thermal budget of neighboring gas particles (Katz 1992; Steinmetz & Muller 1994). In the second one, only a fraction of this energy is allowed to kinetically affect the surrounding particles. This fraction is a free parameter (Navarro & White 1993; Mihos & Hernquist 1994). Both these effects, provided by our code—which is derived from that of Navarro & White (1993)—can solve the overcooling problem described above (Kay et al. 2002).

2.1. *Feedback Strength and Initial Mass Function*

In our model, a fraction (f_v) of SNe energy is supplied to neighboring gas particles in the form of kinetic energy, with the rest $(1 - f_v)$ being added as heat. To be specific, the kinetic energy implementation, due to the number of massive stars that are exploding as SNe during each time step per stellar generation, $\Delta N_*(M > 8\ M_\odot)$, is given by $\Delta E_{\rm SNe,\ vel}(\text{ergs g}^{-1}) = f_v \eta$, where $\eta \simeq 5 \times 10^{17}\ \Delta N_*(M > 8\ M_\odot)/M_*$, and M_* is the mass of a stellar generation that corresponds to a star particle. We point out that the value of the ratio $\Delta N_*(M > 8\ M_\odot)/M_*$ depends on the IMF parameters. Here we assume $f_v = 0.01$ as our fiducial value. In Paper I, we analyzed the role of different IMF parameters on the feedback strength, $\Delta E_{\rm SNe,\ vel}$. As in that paper, B1 simulations correspond to $\alpha = 2.5$, $M_{\rm low} = 0.1\ M_\odot$, and $M_{\rm up} = 100\ M_\odot$ (Miller & Scalo 1979), B2 to $\alpha = 2.35$ with the same mass limits, and B3 models to B2's parameters, but with the lower mass limit, $0.01\ M_\odot$ (Salpeter 1955). Using our self-consistent approach to account for feedback effects, we deduce that B1 models provide a feedback strength 33% higher than the B3 models, whereas B2 models provide a strength 37% higher than B1 and 58% higher than B3 models.

2.2. *The Initial Configuration*

The initial configuration, i.e., the density distribution ($\rho \propto r^{-1}$), the spin parameter, λ (Barnes & Efstathiou 1987) aligned with the shorter principal axis of the DM halo, and the triaxiality ratio of the DM halo as detached by the Hubble flow in a cold dark matter (CDM) scenario, $\tau = (a^2 - b^2)/(a^2 - c^2)$ (Warren et al. 1992) where $a > b > c$, are built up as described in Paper I. Here we assume $\tau = 0.58$ as our fiducial value but the effect of slightly oblate ($\tau = 0.45$) and prolate ($\tau = 0.84$) halos also have been investigated. Different λ values are considered to give insight into the role of the dynamical state of the halo on the evolution of the baryonic matter. All the simulated systems have the same initial virial ratio (0.1) and the same average density to avoid a different collapse time. The total initial number of particles ranges between 2000, as in Paper I, and 20,000, with $N_{\rm DM} = N_{\rm gas}$. We follow the system evolution up to 15 Gyr: the final number of particles ranges from 10,000 to 200,000. The comparison of the results will allow us to analyze in detail the effect of a greater particle resolution. All the simulations performed include self-gravity of gas, stars, and DM, radiative cooling, hydrodynamical pressure, shock heating, artificial viscosity, SF, and feedback from evolved stars and Type II SNe.

3. THE STAR FORMATION RATE AND THE ROTATIONAL SUPPORT OF THE BARYONIC SYSTEM

We find that for a given value of the baryonic–to–total mass ratio, the total mass of the system, $M_{\rm tot}$ ($10^{10}\ M_\odot$ in our units), controls the SFR. Figure 1 (*left panel*) shows that in systems with larger $M_{\rm tot}$, the SF onset arises earlier on and the SFR achieves higher values than in the less massive halos. In the same figure, the effect of a different IMF is also shown. B3 models allow higher SFR as a consequence of their lower feedback strength (see § 2.1). Numerical resolution slightly affects the SFR: the other parameters remain the same (Fig. 1, *right panel*). In Figure 2, we compare the evolution of the rotational support of the baryons for some simulation in Figure 1. We can see that the feedback strength strongly affects the dynamical evolution of the luminous matter (Fig. 2). This is because the lower the SFR, the larger the fraction of cold ($T < 10^5$ K) rotating gas and the lower the amount of random motions induced by the kinetic feedback. In Figure 2 (*left panel*), we examine the behavior of different particle resolution runs, with the other parameters remaining the same. We deduce that the rotational support of the baryons increases with the rising

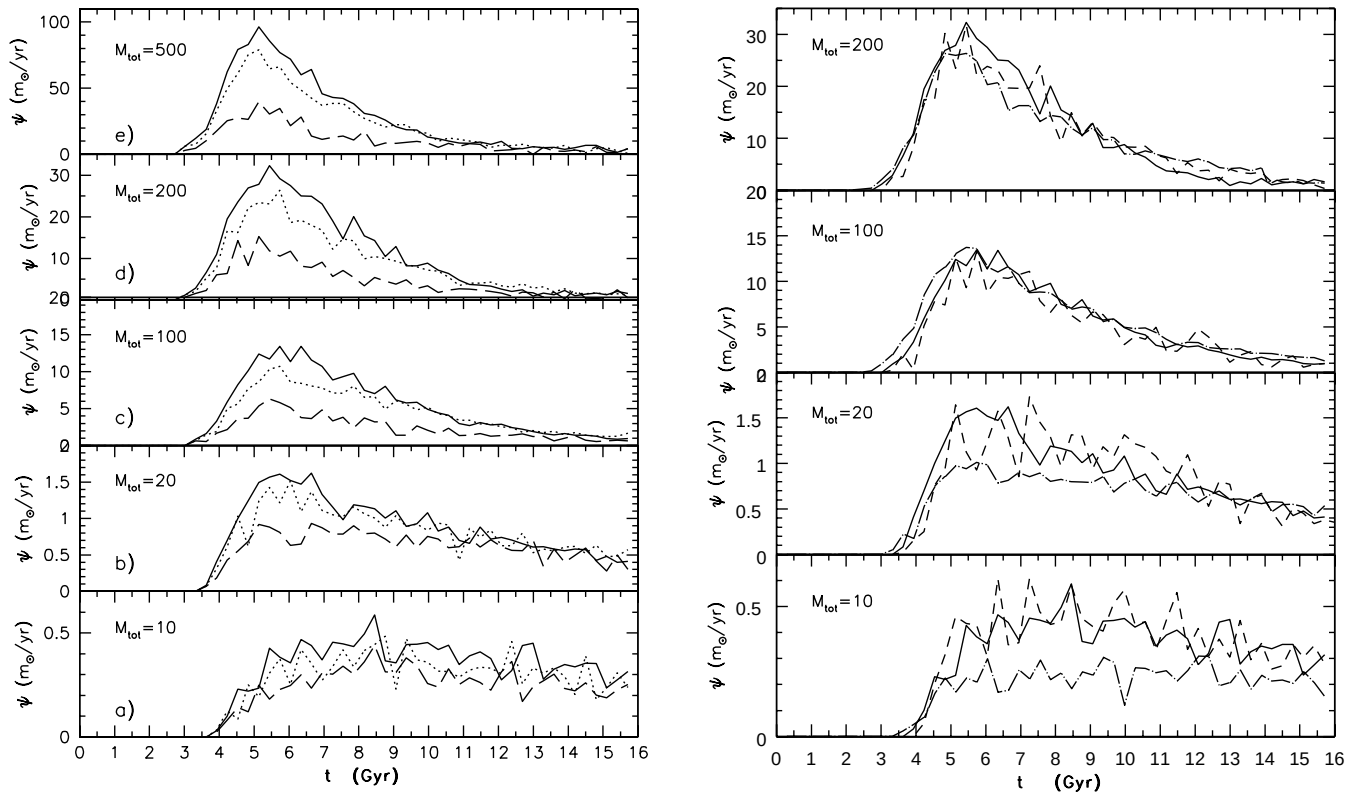


FIG. 1.—*Left*: Time behavior of the SFR for models with 6000 initial particles, $M_{\rm bar}/M_{\rm tot}$ ratio equal to 0.1 but different $M_{\rm tot}$ and different IMF parameters (see text): B1 models (*dotted line*), B2 models (*long-dashed line*), B3 models (*continuous line*). *Right*: Same for B3 models, with different initial particles: 6000 (*continuous line*), 2000 (*short-dashed line*), and 20,000 (*dot-dashed line*). [*See the electronic edition of the Journal for a color version of this figure.*]

resolution, allowing the value expected for local spirals ($\geq$80%; Paper I) for a resolution of at least 6000 initial total particles. Even if the SFR and, therefore, the fraction of residual gas are slightly dependent on particle resolution, that of cold gas is decreased by 10% by reducing gas resolution from 3000 to 1000 particles. This is a very important point: lower resolution could strongly affect the results of cosmological simulations of galaxy formation provided by such feedback. The so-called angular momentum crisis, which together with overcooling is one of the major

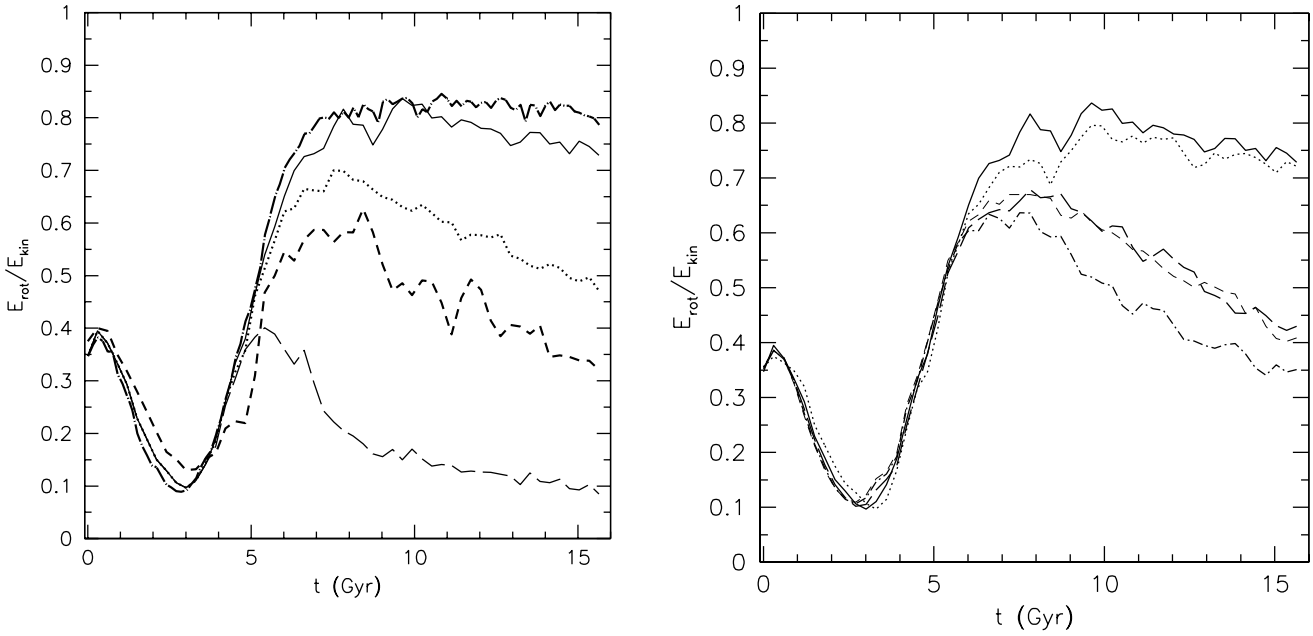


FIG. 2.—Evolution of the rotational support of gas+stars for some models in Fig. 1. *Left*: Effect of different IMF parameters and particle resolution for $M_{\rm tot} = 20$ with the same symbols as in Fig. 1. *Right*: Same for B3 models, with different $M_{\rm tot}$: $M_{\rm tot} = 10$ (*dotted line*), $M_{\rm tot} = 20$ (*continuous line*), $M_{\rm tot} = 100$ (*long-dashed line*), $M_{\rm tot} = 200$ (*dot-dashed line*), $M_{\rm tot} = 500$ (*short-dashed line*). [*See the electronic edition of the Journal for a color version of this figure.*]

TABLE 1
MODELS WITH $M_{\rm tot} = 20$ AND $M_{\rm tot}/M_{\rm bar} = 0.1$

IMF[a]	N_p[b]	$r_{\rm eff}$[c]	r_D[d]	$r_{\rm opt}$[e]	B/D[f]
B1	6000	3.23	4.4	12.82	0.50
B2	6000	2.78	3.5	10.56	0.70
B3	6000	4.00	4.7	13.21	0.43
B3	2000	3.03	4.5	13.09	0.47
B3	20,000	4.18	5.0	12.76	0.44

[a] See text for IMF parameters of different models.
[b] Total initial number of particles.
[c] B effective radius (kpc) as derived by our EPS models (Curir & Mazzei 1999).
[d] Exponential disk scale length (kpc) from B surface brightness distribution.
[e] Optical radius (kpc), i.e., where $L = 0.83 L_{B_{\rm tot}}$ (Salucci & Persic 1997).
[f] Bulge/disk ratio from x-y projection of B surface brightness distribution inside $r_{\rm opt}$.

challenges of cosmological simulations, could be solved accounting for both feedback and high particle galaxy resolution. Our findings agree with recent results of Governato et al. (2002). Taking into account our previous discussion, a suitable choice of IMF parameters (B3 models) could further improve this point. Moreover, we find (Fig. 2, *right*) that our fiducial $M_{\rm bar}/M_{\rm tot}$ ratio gives rise to massive baryon systems with lower rotational support than the less massive ones. In particular, accounting for the dependence of the feedback strength on the IMF parameters claimed above, B3 simulations with $M_{\rm tot} \leq 100$ are most suitable to match the general properties of spirals, whereas more massive systems are required to match those of ellipticals. In Paper I, we derived integrated colors, luminosities, and metallicities, together with mass-to-light ratios, disk scale lengths, etc., of simulated galaxies from 2000 initial particle runs. Photometric integrated properties of a galaxy depend only on its SFR for a given IMF choice (Sandage 1986; Mazzei et al. 1992, 1994). These are not affected by different particle resolution according to the slight dependence of the SFR on such a resolution as outlined above. Table 1 summarizes disk scale lengths and bulge/disk ratios derived for models in Figure 2 (*left*). Such quantities are indeed also affected by the rotational support of the model and, thus, on the resolution of the simulated galaxy. These results translate into important issues concerning morphological types, in particular, spiral galaxies within the very simple framework of monolithic collapse. Our conclusions here, based on the behavior of the SFR and on the rotational support achieved by simulated systems, are moreover fully consistent with photometric integrated properties of local galaxies of different morphological types.

3.1. *The Mass Gas Resolution*

The rise of the SFR with the $M_{\rm tot}$ cited above requires, however, further investigation since by keeping constant the number of initial particles and the $M_{\rm bar}/M_{\rm tot}$ ratio, more massive systems entail more massive gas clouds, thereby raising the efficiency of SF, ϵ, i.e., the fraction of each gas cloud turned into stars (Navarro & White 1993). Thus, we performed several simulations by changing $M_{\rm tot}$ but keeping constant $M_{\rm bar}$, with the aim of resolving the same mass of gas. For this new set of simulations, the gas mass resolution ranges from $3.33 \times 10^6\ M_\odot$ to $6.67 \times 10^7\ M_\odot$: the lower resolution is better than that achieved by Steinmetz & Navarro (2002; $1.27 \times 10^7\ M_\odot$) and like that of Abadi et al. (2002; $3.29 \times 10^6\ M_\odot$). These runs have been performed with 6000 total initial particles. Results of B3 simulations with $M_{\rm bar} = 2$ and a gas resolution $6.6 \times 10^6\ M_\odot$ are presented in Figure 3. We find that the SFR depends on the DM mass, in the sense that the SFR turns on later the larger the $M_{\rm DM}$; however, its maximum value is only slightly lower (Fig. 3, *left panel*). Looking at the dynamical evolution of the baryons (Fig. 3, *right panel*), we find that our fiducial $M_{\rm bar}/M_{\rm tot}$ ratio entails the largest rotational support. The

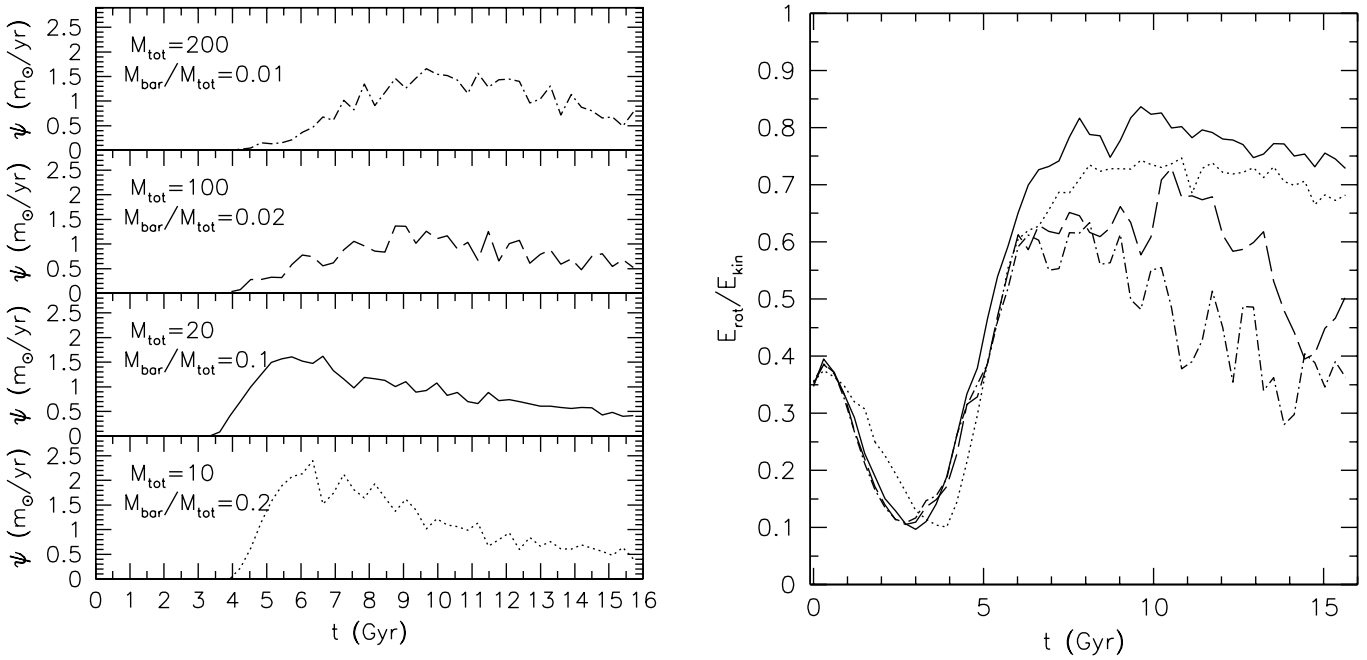


FIG. 3.—*Left*: Evolution of the SFR for B3 models with $M_{\rm bar} = 2$ (see text). *Right*: Rotational support achieved by the baryons in the same models with the same symbols. [*See the electronic edition of the Journal for a color version of this figure.*]

growth (decrease) of DM mass, which reduces (increases) this ratio below (beyond) its fiducial value, also reduces the rotational support of the baryons inside the system (Fig. 4). Thus, we find that the rotational support of the simulated galaxy is also strongly dependent on the value of the $M_{\rm bar}/M_{\rm tot}$ ratio. To conclude our check, we have performed some simulations with the same $M_{\rm bar}/M_{\rm tot}$ ratio but different total masses and ϵ values, such that the same mass of each gas cloud turns on in a star particle. So a simulation with $M_{\rm tot}$ equal to 200 and ϵ equal to 0.04 has to be compared with one having $M_{\rm tot} = 20$ and $\epsilon = 0.4$ (our fiducial value; cf. Fig. 5*c* [*long-dashed lines*] with Fig. 5*a* [*continuous line*]). We deduce that mass gas resolution does not strongly affect our results. For a given $M_{\rm tot}$, the SFR does not depend on such a resolution or the efficiency of SF but is driven by the initial amount of gas. Systems initially gas-depleted show both longer delays of the SF onset, given the lower gas density achieved by the collapsing system, and lower SFRs.

3.2. *The Initial Geometry and Dynamical State of the DM Halo*

A new and interesting point suggested by our work is that galaxy formation and evolution is strongly affected by the initial geometry of the DM halo. For a given $M_{\rm tot}$ and $M_{\rm bar}/M_{\rm tot}$ ratio, the lower the τ, the higher the SFR (Fig. 5*a*). This means that less favorable conditions to the SFR occur inside prolate halos ($\tau > 0.66$), the other parameters being the same. Moreover, the rotational support of the galaxy also depends on this parameter (Fig. 5*b*). We believe that conditions unfavorable to spiral galaxy formation arise inside prolate halos. All the simulations discussed here have been built up with the initial spin parameter, λ, equal to 0.057. To give insight into the effects of a different initial dynamical state on the system evolution, we performed simulations with different λ values. The SF turns on later in systems with a higher λ, which host galaxies endowed with lower rotational support (Fig. 6). Therefore, inside strongly rotating halos, spiral galaxy formation can be suppressed.

4. CONCLUSIONS

In this paper, we analyze the SFR and the rotational support of the simulated galaxies provided by our SPH simulations of isolated collapsing triaxial systems initially composed of DM and gas, with star formation and feedback self-consistently accounted for. We find important connections between dark and luminous matter. The total mass of the system, the DM halo initial geometry, and its dynamical state, drive the galaxy formation and evolution. For a given value of the $M_{\rm bar}/M_{\rm tot}$ ratio, systems with larger $M_{\rm tot}$ turn on the SF earlier, and their SFR achieves higher values than in the less massive halos. Moreover, the baryon's rotational support in the more massive systems is lower than in the less massive halos. Thus, more suitable conditions for elliptical galaxy formation arise in the most massive systems, while in the less massive ones, spirals are favored. Furthermore, we emphasize the effect of different values of the baryonic–to–total mass ratio, $M_{\rm bar}/M_{\rm tot}$, showing that its cosmological value (around 0.1), coupled with the less massive halos, provides the larger rotational support for the simulated galaxy. By changing this ratio for a given $M_{\rm tot}$, we reduce the rotational support of the galaxy. Thus, there are no constraints for the total mass of the system hosting an elliptical galaxy. Our findings shed light on the results of galaxy formation in a fully consistent cosmological scenario (Steinmetz & Navarro 2002; Abadi et al. 2002; Governato et al. 2002) and

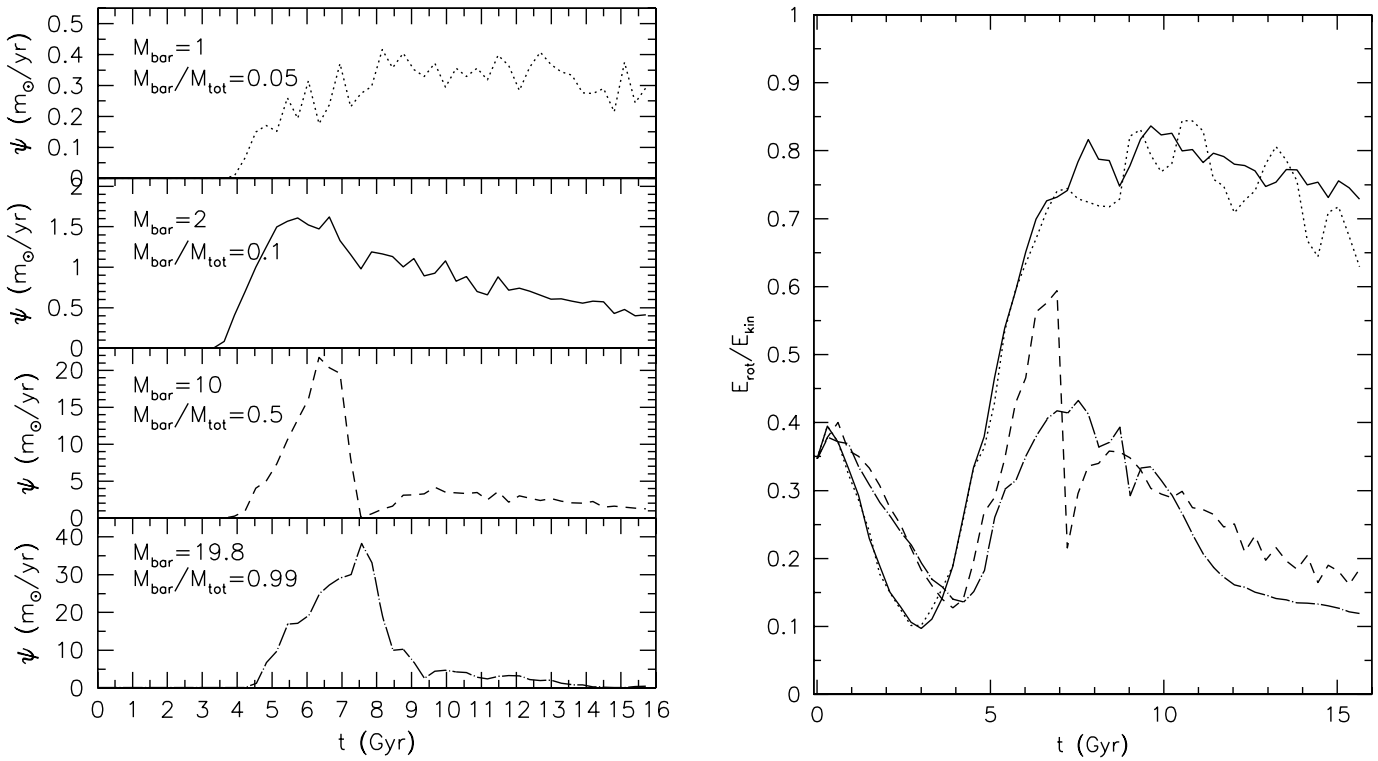


FIG. 4.—*Left*: Evolution of the SFR for B3 models with $M_{\rm tot} = 20$ and different DM mass (see text). *Right*: Rotational support achieved by the baryons in the same models with the same symbols is shown. [*See the electronic edition of the Journal for a color version of this figure.*]

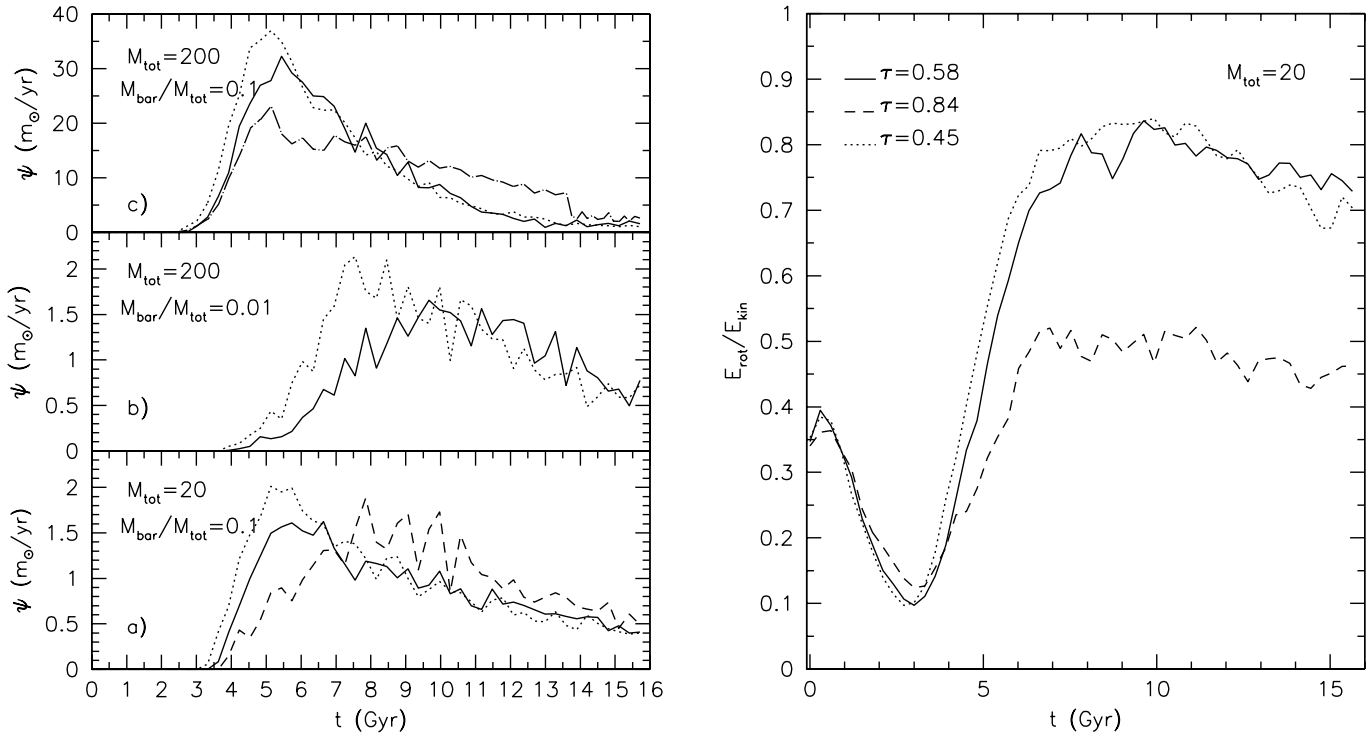


FIG. 5.—*Left panel*: Time behavior of the SFR for B3 models with our fiducial $M_{\rm bar}/M_{\rm tot}$ ratio and different initial τ: oblate halo ($\tau = 0.45$; *dotted line*), triaxial halo ($\tau = 0.58$; *continuous line*), and prolate halo ($\tau = 0.84$; *short-dashed line*). (*c*) $\epsilon = 0.04$ (*dotted, long-dashed line*; see text). *Right panel*: Evolution of rotational support of B3 models in (*a*, *left*). [*See the electronic edition of the Journal for a color version of this figure.*]

raise important issues concerning morphological types—spiral galaxies, in particular—within the very simple framework of monolithic collapse. These are $M_{\rm tot} \leq 10^{12}\ M_\odot$ and $M_{\rm bar}/M_{\rm tot} = 0.1$. In this framework, moreover, prolate shapes of the collapsing halos with high spin parameters ($\lambda \geq 0.06$) delay the onset of the SF process, reduce the star formation activity, and provide baryon systems with lower rotational support. We show that the SFR is not affected by gas particle resolution which, in its turn, slightly affects the feedback strength by reducing the fraction of hot clouds with increasing resolution. Thus, chemophotometric integrated properties of our simulated galaxies (Paper I) are not changed by improving resolution. However, they can be affected by the dust amount and distribution. This will be

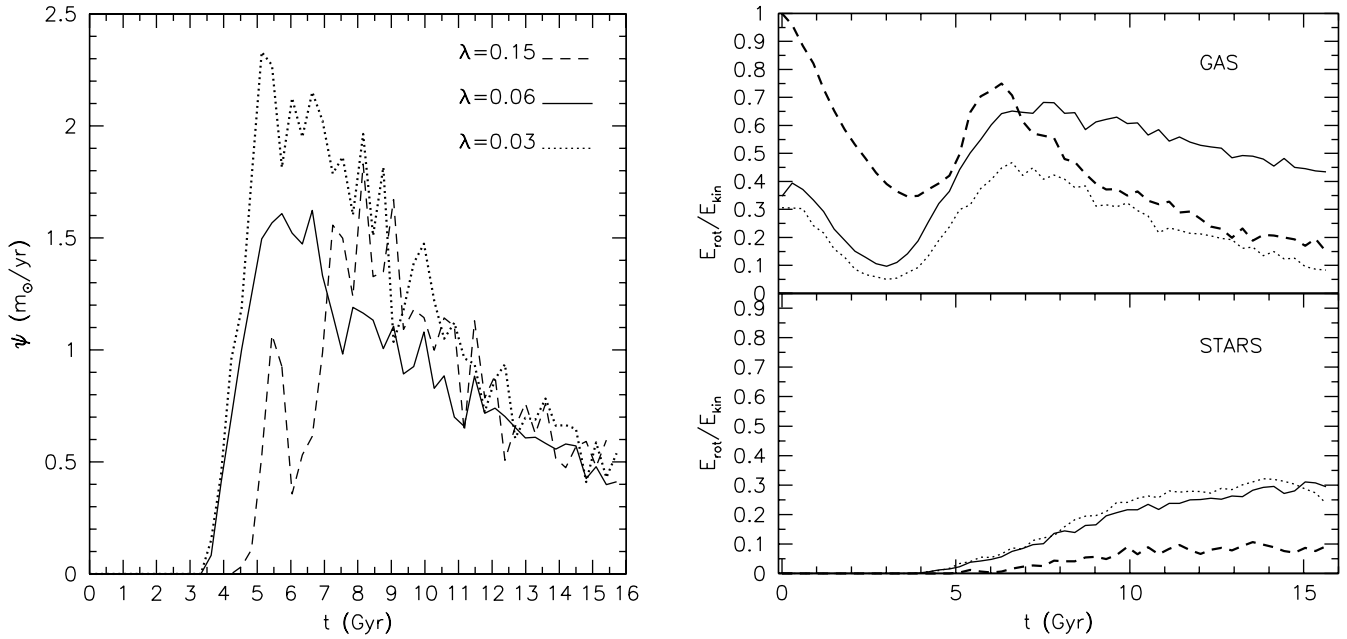


FIG. 6.—*Left*: Evolution of the SFR for B3 models with $M_{\rm tot} = 20$ and our fiducial value of $M_{\rm bar}/M_{\rm tot}$ ratio for different values of the initial spin parameter, λ. *Right*: Corresponding rotational support for stars and gas. [*See the electronic edition of the Journal for a color version of this figure.*]

analyzed in a forthcoming paper. The rotational support of the galaxy is strongly dependent both on the feedback strength and resolution. A suitable IMF choice that controls the feedback strength improves this point further. Therefore, the so-called angular momentum crisis, one of the major challenges of cosmological simulations, could be solved accounting for both feedback and high gas particle resolution.

We are grateful to an anonymous referee whose comments helped us to further improve this paper.

REFERENCES

Abadi, G. M., Navarro, J. F., Steinmetz, M., & Eke, V. R. 2002, ApJ, submitted (astro-ph/0211331)
Barnes, J., & Efstathiou, G. 1987, ApJ, 319, 575
Barnes, J., & Hernquist, L. 1991, ApJ, 370, L65
Curir, A., & Mazzei, P. 1999, NewA, 4, 1 (Paper I)
Governato, F., et al. 2002, ApJL, submitted (astro-ph/0207044)
Katz, N. 1992, ApJ, 391, 502
Katz, N., Hernquist, L., & Weinberg, D. H. 1992, ApJ, 399, L109
Katz, N., Weinberg, D. H., & Hernquist, L. 1996, ApJS, 105, 19
Kay, S. T., Pearce, F. R., Frenck, C. S., & Jenkins, A. 2002, MNRAS, 330, 113
Mazzei, P., De Zotti, G., & Xu, C. 1994, ApJ, 426, 97
Mazzei, P., Xu, C., & De Zotti, G. 1992, A&A, 256, 45
Mihos, J. C., & Hernquist, L. 1994, ApJ, 437, 611
Miller, G. E., & Scalo, J. M. 1979, ApJS, 41, 513
Navarro, J. F., & White, S. D. M. 1993, MNRAS, 265, 271
———. 1994, MNRAS, 267, 401
Salpeter, E. E. 1955, ApJ, 121, 161
Salucci, P., & Persic, M. 1997, in ASP Conf. Ser. 117, Dark Halos around Galaxies, ed. M. Persic & P. Salucci (San Francisco: ASP), 1
Sandage, A. 1986, A&A, 161, 89
Springel, V. 2000, MNRAS, 312, 859
Steinmetz, M., & Muller, E. 1994, A&A, 281, 71
Steinmetz, M., & Navarro, J. F. 2002, NewA, 7, 155
Warren, M. S., Quinn, P. J., Salomon, J. K., & Zurek, W. H. 1992, ApJ, 399, 405
White, S. D. M., & Rees, M. J. 1978, MNRAS, 183, 341